NANO LETTERS

Letter

pubs.acs.org/NanoLett

Electrical Transport Measured in Atomic Carbon Chains

Ovidiu Cretu,[†] Andrés R. Botello-Mendez,[‡] Izabela Janowska,[§] Cuong Pham-Huu,[§] Jean-Christophe Charlier,[‡] and Florian Banhart*[,†]

[†]Institut de Physique et Chimie des Matériaux, Université de Strasbourg, UMR 7504 CNRS, 23 rue du Loess, 67034 Strasbourg, France

[‡]Institute of Condensed Matter and Nanosciences, Université Catholique de Louvain, Chemin des étoiles 8, 1348 Louvain-la-Neuve, Belgium

[§]Institut de Chimie et Procédés pour l'Energie, l'Environnement et la Santé, UMR 7515 CNRS, 25 rue Becquerel, 67087 Strasbourg, France

Supporting Information

ABSTRACT: The first electrical-transport measurements of monatomic carbon chains are reported in this study. The chains were obtained by unraveling carbon atoms from graphene ribbons while an electrical current flowed through the ribbon and, successively, through the chain. The formation of the chains was accompanied by a characteristic drop in the electrical conductivity. The conductivity of the chains was much lower than previously predicted for ideal chains. First-principles calculations using both density functional and many-body perturbation theory show that strain in the chains has an increasing effect on the conductivity as the length of the chains increases. Indeed, carbon chains are always under varying nonzero strain that transforms their atomic structure from the *cumulene* to the *polyyne* configuration, thus inducing a tunable band gap. The modified electronic structure and the characteristics of the contact to the graphitic periphery explain the low conductivity of the locally constrained carbon chain.

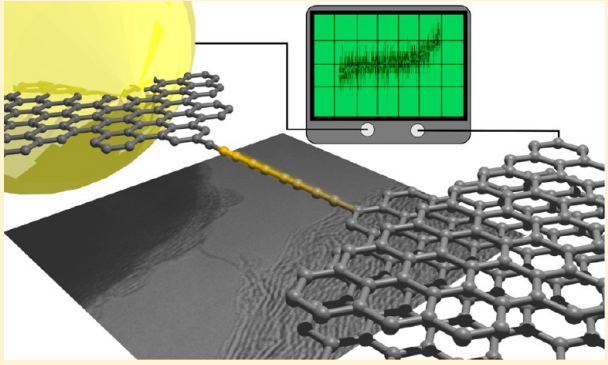

KEYWORDS: *Atomic carbon chains, atomic wires, carbynes, electron microscopy, quantum transport*

Reducing carbon materials from three to two dimensions has revealed a new world of physical phenomena and technological applications in the past few years. However, graphene as the two-dimensional allotropic form of carbon is not necessarily the lowest limit of spatial confinement. Narrow strips of graphene or small carbon nanotubes are already quasi one-dimensional (1D) systems exhibiting 1D signatures. However, linear chains of atoms are the thinnest imaginable and the only real 1D allotropic form of carbon.[1] There had been many speculations about the existence and stability of *pure* atomic carbon chains[2] and about their properties until these 1D objects were finally observed in the electron microscope.[3−6] Indications for carbon chains have also been given, for example, in the field emission characteristics of carbon nanotubes,[7] in the electrical properties of a breaking nanotube,[8] or during the coalescence of heat-treated carbon nanotubes.[9] However, these measurements could not yet be considered as direct evidence for the existence of carbon chains.

Theoretical studies have predicted interesting properties for pure atomic carbon chains. Indeed, an ideal carbon chain, also called cumulene, is characterized by σ-bonds along the axis (e.g. $s-p_x$ orbitals), and two decoupled π-bonds per atom from the perpendicular p_y and p_z orbitals. Similarly to higher-dimension carbon allotropes, both σ- and π-bonds in carbon chains are predicted to result in outstanding mechanical properties, for example, a Young's modulus of more than 1 order of magnitude higher than diamond,[10] as well as in a specific metallic behavior. However, this 1D system is subject to Peierls's instability, leading to a distorted lattice with bond length alternation (i.e., dimerization) and the appearance of a band gap.[11] This semiconducting behavior characterizes the polyyne configuration whose conductivity has been predicted to oscillate depending on an even or odd number of atoms in the chain.[12,13] Furthermore, polyyne should exhibit spin-dependent transport properties.[14] Since the energetic stability difference between the perfect system (*cumulene*, with double bonds throughout the chain, =C=C=C=C=C=) and the distorted system (*polyyne*, with alternating single and triple bonds, —C≡C—C≡C—C≡) is rather small,[15] both 1D systems could coexist under appropriate experimental conditions. Therefore, carbon chains can be considered as ideal one-dimensional conductors and could find application as the thinnest possible wires for interconnecting ultimate nanodevices.

Received: March 1, 2013
Revised: July 9, 2013

   dx.doi.org/10.1021/nl4018918 | *Nano Lett.* XXXX, XXX, XXX−XXX

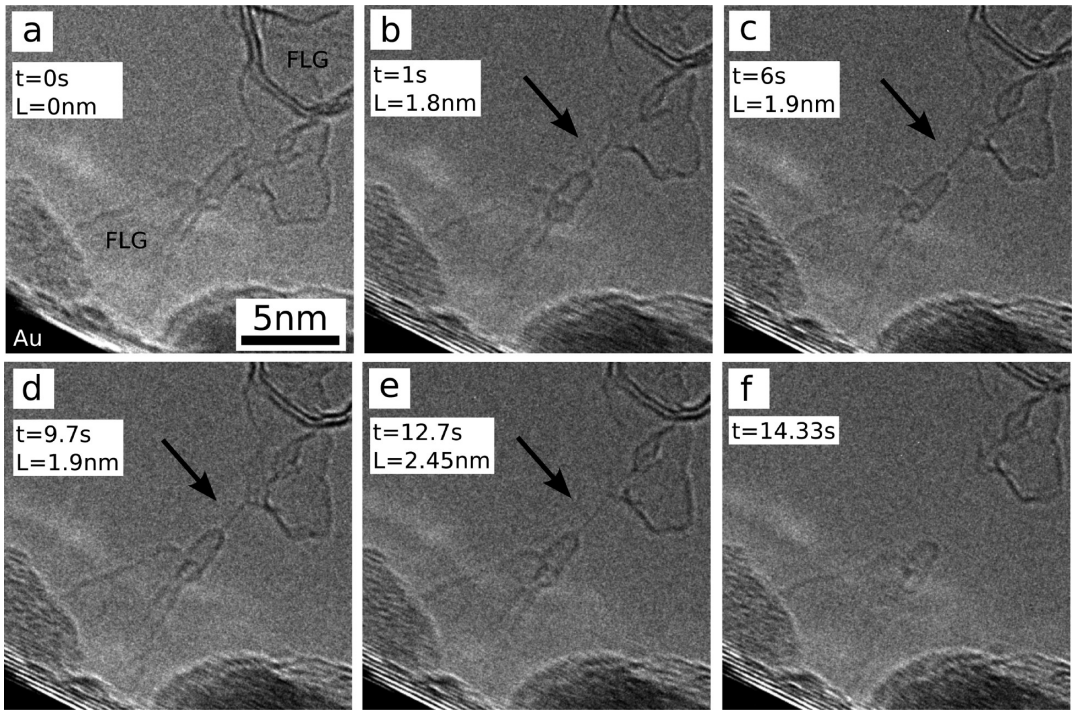

Figure 1. In situ synthesis of a monatomic carbon chain. (a) A few-layer graphene nanoribbon (FLG) breaks and forms a carbon chain (arrowed) which is stable for a few seconds (b−e). The chain eventually breaks and disconnects the two FLG regions (f). The time scale as well as the measured length of the chain (in the projection onto the image plane) are indicated.

Notwithstanding the interest in carbon chains, their electrical properties have not been measured hitherto due to the difficulty of synthesizing and contacting these unstable objects. Here, by using a scanning tunneling microscopy (STM) tip in a transmission electron microscopy (TEM) stage, both the synthesis and the electrical characterization of free-hanging atomic carbon chains are carried out in situ. Surprisingly, their capability to carry an electrical current turned out to be much lower than expected and is explained using state-of-the-art electronic-structure and quantum-transport calculations performed on specific configurations.

Few-layer graphene was obtained by the mechanical ablation of pencil lead, assisted by ultrasonification and followed by an acid/base purification.[16] The graphene flakes had a small number of layers and an average lateral size of 2 μm. Iron nanoparticles with an average size of 5 nm were deposited on the graphene flakes, leading to a catalytic cutting of the sheets. Pure iron and iron carbide particles as well as iron particles encapsulated in graphitic shells were obtained (details of the preparation procedure are described in the Supporting Information). After dispersing the material in ethanol, a few drops of the suspension were deposited on a holey carbon TEM grid which had been previously cut in two halves. One of the half-grids was then mounted in a NanoFactory TEM sample holder[17,18] that allows contacting exposed parts of the sample by precisely positioning an STM tip onto their surfaces. Gold tips prepared by electrochemical etching[19] were used as contacts. After establishing a contact between the Au tip and the half-grid, an electrical bias was applied between the sample and the tip, and the resulting current was measured. The electrical measurements were monitored and recorded in real-time together with TEM images or videos of the contact region, giving a complete picture of the process. Under these operating conditions, the resolution of the microscope was around 0.2 nm, while the current through the system was measured at the same time with a precision of the order of 1 nA. The temporal resolution for imaging and simultaneous electrical measurements was of the order of 0.1 s. Images of the graphene flakes show a series of straight bands due to the interaction between the Fe nanoparticles and the graphene layers over which the Fe particles migrate.[20] The cutting of the flake by the moving Fe crystals leads to the formation of thin graphene nanoribbons standing off the edges (c.f. Figure S1 of the Supporting Information). These graphene ribbons were used as precursors for the formation of monatomic carbon chains.

The in situ synthesis of a carbon chain is summarized in Figure 1 (see Supplementary Movie 1). The process started by contacting the edge of a few-layer graphene sheet with a Au tip. The first step was to ensure a good contact, which was either done by gradually increasing the voltage until the current through the circuit reached several 10^{-4} A; typically at voltages around 1−1.5 V. Alternatively, the voltage was increased abruptly to higher values (2−3 V) while the current was limited to some 10^{-4} A in order to prevent the destruction of the graphene layers. Once such an electrical contact had been achieved, the voltage was decreased to around 1 V, and the tip was retracted slowly. As the part of the sample which is in contact with the tip starts to break from the larger flake, graphitic structures of less than 1 nm in width were formed between the two regions; this can be seen in Figure 1a. Further separation of the tip from the sample resulted in the formation of a stretched graphenic structure (either flat or tube-like) and, eventually, in the unraveling of a monatomic carbon chain from the graphenic layer (Figure 1b). Under these conditions, the chain was found to be stable for a few seconds (Figure 1b−e). The chain eventually broke and interrupted the electrical circuit (Figure 1f). However, in most attempts the graphene ribbon

dx.doi.org/10.1021/nl4018918 | *Nano Lett.* XXXX, XXX, XXX−XXX

detached completely from one of the electrodes without forming a chain.

Each time when a chain unraveled from a graphenic structure, a characteristic drop of the electrical current was observed. Two examples are presented in Figures 2a and b. The

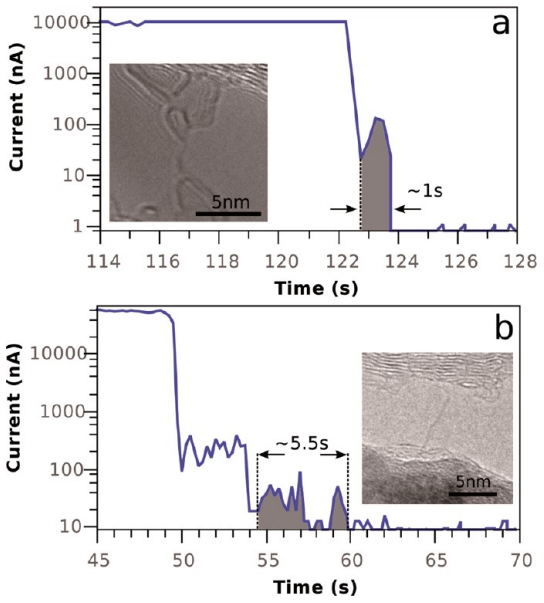

Figure 2. Electrical current through two (a, b) monatomic carbon chains at a constant bias of 1 V. The evolution of the current, monitored at the formation of the two chains, is shown (blue curve). The filled regions under the curve correspond to the periods where the chains appeared. The image insets show the respective chains. The saturation of the current in the first part of a is the result of setting a ~10 μA current limit.

current drops abruptly from several 10^{-5} A (graphene ribbon) to values in the range 10^{-7}–10^{-9} A (atomic chain). The low current persists for a few seconds and then drops to zero when the chain breaks and the circuit is eventually interrupted. By synchronizing the videos with the electrical recordings, it was found that the formation of the chains corresponds exactly to the moment where the current drops from micro- to nanoamperes. The low-current regime corresponds to the lifetime of the chains. This evolution was typical for all chains that were observed. The drop in current when the chain is formed proves that the linear contrast features are not projections of graphene ribbons in side-view. Measurements on narrow graphene ribbons, that were also obtained in some of the experiments, show a conductivity orders of magnitude higher than the atomic chains. In view of earlier discussions about the nature of the linear contrast (atomic chains vs ribbons in side-view),[4,5] this supports the fact that atomic chains are clearly present.

The short lifetime of the chains only allowed the recording of current–voltage characteristics in a few cases. Since the recording of an I–V curve was possible within 0.1 s, it was unaffected by the large fluctuations in conductivity that appear in Figure 2. Two I–V measurements for typical chains are presented in Figure 3. Both depict qualitatively similar characteristics as the current changes by only 1–2 nA at a voltage variation of several hundred millivolts. The onset of the current rise occurs at different voltages in the two chains shown here. Although the measurements of the low currents are affected by noise, both curves exhibit clear nonohmic behavior.

The formation of the carbon chains can be explained by the unraveling of atoms from a graphene ribbon or a single-wall carbon nanotube.[7] In the present study, such a process is likely to occur due to the mechanical forces that are deliberately applied to the system. Several theoretical studies have already suggested the possibility of creating atomic carbon chains by inducing strain in graphene at room temperature[21–23] as well as at high temperature.[24] The role that defects in graphene[25] might play in this process has also been emphasized.[4,5] By analyzing the evolution of the chains in the present experiments, a slow but ongoing unraveling of carbon atoms that increases the length of the chains is apparent. This might be responsible for the large fluctuations of current that was observed in most measurements (Figure 2). A length increase of up to 36% was seen which is much higher than the predicted ultimate strain of 12%.[26] Hence, there is evidence that the structures under investigation continuously evolve. However, since different chains present quite different (though small) conductivities, strain in the linear arrangement should play an important role.[15,27]

To investigate the electronic and mechanical coupling in carbon chains, first-principles density functional theory (DFT) and many-body perturbation theory (MBPT) calculations (see Computing Techniques in the Supporting Information) were performed to investigate both the electronic and structural properties in 1D carbon-based systems (Figure 4). The ab initio electronic structure of a cumulene chain exhibits degenerate π

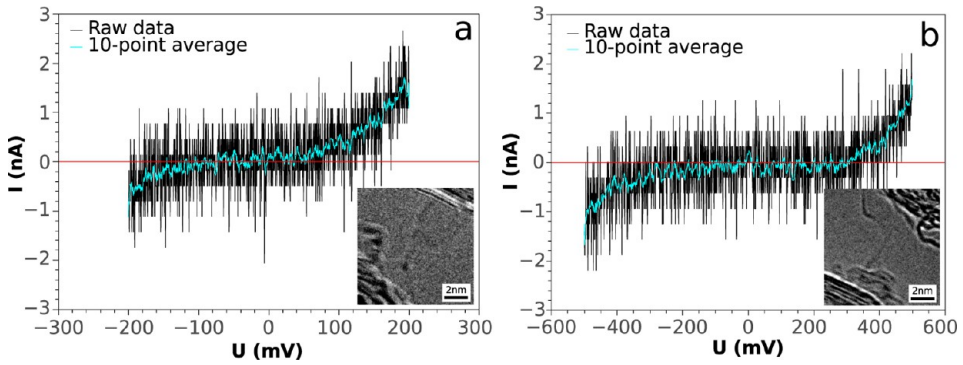

Figure 3. I–V measurements on two monatomic carbon chains (cf., Figure S2). Images of the chains are displayed in the insets (the contrast in a is hardly visible due to the vibration of the chain). The discrete values of the noise are due to the sampling depth of the analog–digital conversion in the current recording.

dx.doi.org/10.1021/nl4018918 | *Nano Lett.* XXXX, XXX, XXX–XXX

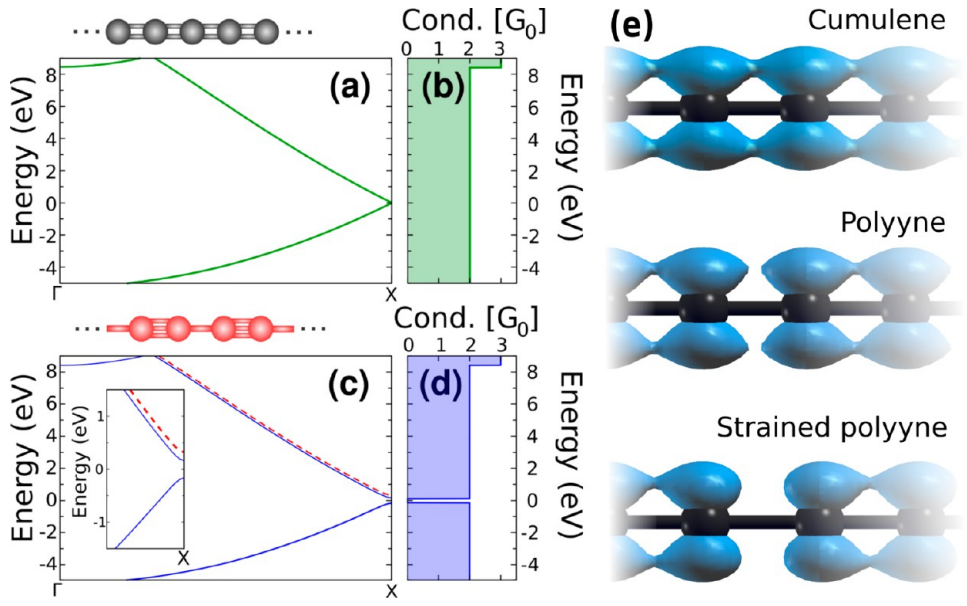

Figure 4. Ab initio electronic structures and quantum conductances of cumulene (a, b) and polyyne (c, d) carbon chains. The inset of c illustrates the band structure of polyyne within DFT/LDA (blue curves) and GW (dotted red line). For more details, see Computing Techniques in the Supporting Information. Electronic distribution (π orbitals in blue) perpendicular to the chain (e) within the two atomic configurations (cumulene and polyyne) and under mechanical strain.

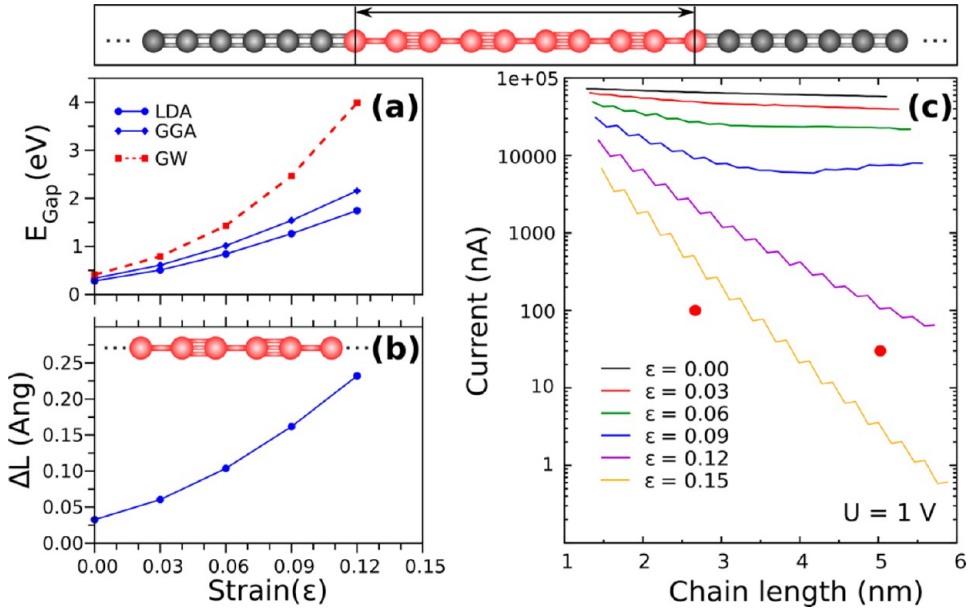

Figure 5. Strain dependence of the atomic structure, the electronic band gap, and electron current in carbon chains. (a) Electronic band gap versus strain in a polyyne chain within the approximations DFT/LDA (blue circles), DFT/GGA (blue diamonds), and GW (red squares). (b) Dimerization (ΔL: length of the longer bond minus length of the shorter one) versus strain in a polyyne chain. (c) Current as a function of length and strain calculated from the integration of quantum conductances of polyyne segments embedded in two ideal cumulene metallic leads (model on top). An applied voltage of 1 V has been assumed. The length of the chain is defined by the red polyyne section (line with double arrows). Two experimental measurements of the current at different lengths of the chain (red points) are plotted for comparison.

bands crossing the Fermi energy (Figure 4a), thus resulting in a quantum conductance of two quanta G_0 ($G_0 = 2e^2/h$) and a corresponding current of 15 μA at 0.1 eV bias (Figure 4b). Within this highly symmetric configuration, the π orbitals are homogeneously distributed along the chain, forming equivalent bonds (Figure 4e, top). As mentioned previously, such an ideal 1D system is subject to structural distortion. Indeed, Peierls's theorem predicts that a 1D system of equally spaced atomic sites with one electron per atom is unstable. A lattice distortion will cause the electrons to be at a lower energy than they would be in a perfect crystal, thus inducing the well-known Peierls dimerization in the chain as can be observed from the plot of the electronic distribution of pi orbitals shown in Figure 4e. This new structure with bond-length alternation (Figure 4e, middle), becomes energetically favorable and, due to the loss of symmetry, exhibits an electronic band gap (E_{Gap}). The LDA (GGA) ab initio electronic structure of this polyyne chain presents an E_{gap} of 0.28 (0.34) eV (Figure 4c). However,

dx.doi.org/10.1021/nl4018918 | Nano Lett. XXXX, XXX, XXX−XXX

although the DFT calculations usually give an efficient and accurate description of ground state properties (total energy, lattice constants, atomic structures, phonon spectra, etc.), the Kohn–Sham band structure systematically underestimates the band gap (often by more than 50%).[28] In order to address excited-state properties and to calculate the band structure including electron–electron interactions (many body effects), MBPT calculations within the GW approximation for the self-energy are frequently used to provide corrected values for E_{Gap} in better agreement with experiments.[29] The value of E_{Gap} for the polyyne chain estimated after the GW corrections to DFT/LDA is 0.407 eV (Figure 4c, dotted red line). Such an absence of electronic states is also clearly visible in the quantum conductance of the polyyne chain (Figure 4d).

Figure 5a illustrates the strain dependence of the electronic band gap (in both DFT and MBPT approaches) for an infinite polyyne chain. Note that 5% strain is enough to induce a 1 eV GW gap. In addition, as the strain increases, the dimerization (ΔL: difference of lengths between the triple and the single bonds in the polyyne chain) is more pronounced (Figure 5b), thus stabilizing this specific configuration under strain.[15] Indeed, the electronic distribution perpendicular to the strained polyyne chain depicts that π-orbitals are even more localized on the shorter bond length than for the pristine polyyne case (Figure 4e, bottom).

To estimate the transport in carbon chains, DFT calculations using open boundary conditions were used to predict the quantum conductance throughout a linear carbon chain.[30] The quantum conductance of the cumulene chain is characterized by two channels due to the two conduction and two valence bands that meet at the edge of the Brillouin zone (BZ) and thus gives a conductance of $2G_0$ (Figure 4a–b). Similarly, the polyyne chain presents a conductance of $2G_0$, except close to the charge neutrality point (Figure 4c–d). Due to the dimerization process inducing two different bond lengths, the loss of symmetry between the carbon atoms lifts the degeneracy between the conduction and the valence bands at the corner of the BZ (see dotted line in the inset in Figure 4c). A 1D system constituted by a polyyne segment embedded into two perfectly conducting semi-infinite cumulene chains (e.g., 10 carbon atoms as depicted in Figure 5) is used as a realistic atomic model of a polyyne chain with seamless contacts. Such a model is used to highlight the effect of strain that could appear locally in the carbon chain. Indeed, a local constraint should stabilize a polyyne-type configuration locally (finite-size segment), thus perturbing transport along the chain. Recall that the DFT conductance does not reflect the predicted GW gap for an infinite polyyne chain under strain. To go beyond this DFT problem, a π–π^* distance dependent tight-binding approach that reproduces the GW band gaps for different strains was used. The quantum conductance for the polyyne segment embedded on semi-infinite cumulene leads was calculated for different chain lengths and strain. An estimation of the current flowing through these systems was obtained by the integration of the quantum conductance from the charge neutrality point to 1 eV considering the charge density at zero bias (Figure 5c and Figure S2). The fluctuations of the current are due to the difference in conductance between an even and odd number of atoms in the atomic chain. The current is found to drop by several orders of magnitude for long chains when the strain increases from 0 to 15%.

A comparison of the predicted currents and the experimental measurements is possible within some limits and illustrated by two experimentally measured values in Figure 5c. However, a precise quantitative comparison remains difficult since the strain cannot be measured experimentally and the lengths of the chains can only be estimated due to projection effects in the images. However, the simulations confirm the experimentally measured currents if we assume longer chains under a strain of approximately 12–15% which appears quite realistic under the present experimental conditions (pulling out of the chains). These strain values are close to the predicted ultimate strain,[26] thus probably explaining the short lifetime of the chain during the transport measurements. Nevertheless, the conductance drop due to strain cannot account for a two orders-of-magnitude drop as observed experimentally for curved chains that should not be strained considerably. Other mechanisms could play an important role. For instance, the conductance should be even lower than stated above if calculated using a self-consistent GW scheme with updated wave functions, which is a highly computer-demanding technique that has recently demonstrated its success[31] although only for small molecular systems. Furthermore, electron–phonon interactions (not taken into account in the present transport calculations) could play an important role as well as the contact resistivity.

Indeed, a key factor determining the electrical transport through a carbon chain is the nature of the contacts between the chain and the electrodes. The carbon chains synthesized in the present study are obtained by breaking larger carbon structures which leads to carbon–carbon bonds at the ends of the chain, as previously investigated theoretically.[32] Furthermore, cases were observed where one end of the chain detached and reconnected repeatedly at one of the graphitic contacts (shown in Figure S3 of the Supporting Information). Here, the end of the chain jumps between different positions on the graphitic support, but the current remains below 200 nA throughout this process, similarly to the "fixed" chains. From the theoretical viewpoint, an accurate treatment of the contacts is challenging because the properties of these systems are very sensitive to the exact geometry of the bond between the chain and the graphitic material.[33,14] However, it can be anticipated that the conductance should drop even more drastically due to interference and reflections that are not considered in the transport calculations presented above. Both the absence of atomistic information regarding the contact between the monatomic chain and the bulk material and the inability of conventional DFT methods to reproduce the conductance measured for even simpler nanojunctions[34] do not allow the prediction of accurate electrical characteristics for the present carbon systems. Nevertheless, the observed large fluctuations of the conductivity during the measurements can most likely be attributed to both changing characteristics of the contacts and changes in strain. Consequently, the upper limits of the measured currents should be taken as realistic values that are less influenced by contact characteristics. The contact resistivities are in series with the resistivity of the chain. As the system is in the steep region of the I/V curve (cf., Figure S2), small changes of local voltage on the chain considerably modify the corresponding current (Figure 2).

The current–voltage characteristics of carbon chains under the above-mentioned conditions were also calculated and are presented in Figure S2 in the Supporting Information. The experimentally measured I–V curves as shown in Figure 3 are in accordance with the calculations for larger strains and lengths of the chains which, in turn, corresponds to the conclusions

dx.doi.org/10.1021/nl4018918 | Nano Lett. XXXX, XXX, XXX–XXX

drawn from the absolute values of the currents at constant voltage (Figure 5c).

The influence of both temperature and electron irradiation has also to be taken into account. Due to the nonuniform structure between the electrodes, the estimation of Ohmic heating is difficult (electron-beam heating is negligible). While we can assume a considerable heating effect in the graphene ribbons[35] before the formation of the chain, the current through the chain itself is low so that heating should occur on a moderate scale. Furthermore, the thermal conductivity of both graphene and carbon chains is supposed to be very high,[36] so the heat should dissipate efficiently toward the bulky electrodes. While electron irradiation does not cause persistent electronic excitations in systems with conduction electrons, ballistic atom displacements may occur.[37] By assuming a displacement threshold of 14 eV,[38−40] we calculated a displacement rate of approximately 0.01 s^{-1} for each carbon atom under the present irradiation conditions. At a chain length of 10 atoms a displacement would occur every 10 s. This is only slightly longer than the observed lifetime of a chain, so we may assume that the observed breakage of the chain may, at least in some cases, be due to the displacement of a carbon atom by the electron beam. Hence, under nonirradiation conditions, the lifetime of the chains might be longer.

The present study shows for the first time that atomic carbon chains exhibit electrical conductivity, albeit lower than predicted for ideal unstrained chains. The low measured conductivity is explained in terms of local strain in the chain but is also due to the contact with the electrodes. Indeed, while measuring the electrical current, atomic carbon chains are always inherently strained and, thus, exhibit a varying but always nonzero bandgap. Since both strain and contact characteristics change considerably during the measurements, the conductivity never reaches the predicted values for ideal chains. In addition, our simulations show that a unique cumulene or polyyne configuration might not exist due to the varying strain and, correspondingly, varying bonding state due to the stabilization of the dimerization process under stress. This result might have important consequences on the understanding of the nature and stability of carbynes and related carbon-based linear structures. Furthermore, the present study shows that the characteristics of the contact between carbon chains and their periphery are difficult to control on the necessary (i.e., atomic) level. Nevertheless, our HRTEM observations indicate the feasibility of recently proposed mechanisms for atomic-scale switches in logical nanodevices.[41] Carbon chains remain interesting candidates for interconnects of subnanometer dimensions. Further applications could be found as 1D sensors since the electronic transport should be drastically affected by adsorbents (such as chemical or biological species that can be attached to the chains) that, besides changing the electronic structure, should also have considerable influence on the strain in the chain.

■ ASSOCIATED CONTENT

Supporting Information

Preparation of the starting material, supplementary figures, computational procedure, and supplementary videos. This material is available free of charge via the Internet at http://pubs.acs.org.

■ AUTHOR INFORMATION

Corresponding Author

*E-mail: florian.banhart@ipcms.unistra.fr.

Present Address

O.C.: National Institute of Advanced Industrial Science and Technology, Central 5, 1-1-1 Higashi, Tsukuba, Ibaraki 305-8565, Japan.

Notes

The authors declare no competing financial interest.

■ ACKNOWLEDGMENTS

Funding by the French *Agence Nationale de Recherche* (project NANOCONTACTS, NT09 507527) is gratefully acknowledged. A.R.B.M. and J.-C.C. acknowledge financial support from the F.R.S.-FNRS of Belgium. This research is directly connected to the ARC on "Graphene Nanoelectromechanics" (no. 11/16-037) sponsored by the Communauté Française de Belgique and to the European ICT FET Flagship entitled "Graphene-based revolutions in ICT and beyond". Computational resources were provided by the CISM of the Université Catholique de Louvain.

■ REFERENCES

(1) Heimann, R. B.; Evsyukov, S. E.; Kavan, L. *Carbyne and Carbynoid Structures*; Kluwer Academic Publishers: Dordrecht, 1999.

(2) Kim, S. G.; Lee, Y. H.; Nordlander, P.; Tománek, D. *Chem. Phys. Lett.* **1997**, *264*, 345.

(3) Troiani, H. E.; Miki-Yoshida, M.; Camacho-Bragado, G. A.; Marques, M. A. L.; Rubio, A.; Ascencio, J. A.; Jose-Yacaman, M. *Nano Lett.* **2003**, *3*, 751.

(4) Jin, C.; Lan, H.; Peng, L.; Suenaga, K.; Iijima, I. *Phys. Rev. Lett.* **2009**, *102*, 205501.

(5) Chuvilin, A.; Meyer, J. C.; Algara-Siller, G.; Kaiser, U. *New J. Phys.* **2009**, *11*, 083019.

(6) Börrnert, F.; Börrnert, C.; Gorantla, S.; Liu, X.; Bachmatiuk, A.; Joswig, J.-O.; Wagner, F. R.; Schäffel, F.; Warner, J. H.; Schönfelder, R.; Rellinghaus, B.; Gemming, T.; Thomas, J.; Knupfer, M.; Büchner, B.; Rümmeli, M. H. *Phys. Rev. B* **2010**, *81*, 085439.

(7) Rinzler, A. G.; Hafner, J. H.; Nikolaev, P.; Lou, L.; Kim, S. G.; Tománek, D.; Nordlander, P.; Colbert, D. T.; Smalley, R. E. *Science* **1993**, *269*, 1550.

(8) Yuzvinsky, T. D.; Mickelson, W.; Aloni, S.; Begtrup, G. E.; Kis, A.; Zettl, A. *Nano Lett.* **2006**, *6*, 2718.

(9) Fantini, C.; Cruz, E.; Jorio, A.; Terrones, M.; Terrones, H.; Van Lier, G.; Charlier, J.-C.; Dresselhaus, M. S.; Saito, R.; Kim, Y. A.; Hayashi, T.; Muramatsu, H.; Endo, M.; Pimenta, M. A. *Phys. Rev. B* **2006**, *73*, 193408.

(10) Itzhaki, L.; Altus, E.; Basch, H.; Hoz, S. *Angew. Chem.* **2005**, *117*, 7598.

(11) Saito, R.; Dresselhaus, G.; Dresselhaus, M. S. *Physical Properties of Carbon Nanotubes*; Imperial College Press: London, 1998.

(12) Lang, N. D.; Avouris, Ph. *Phys. Rev. Lett.* **1998**, *81*, 3515.

(13) Khoo, K. H.; Neaton, J. B.; Son, Y. W.; Cohen, M. L.; Louie, S. G. *Nano Lett.* **2008**, *8*, 2900.

(14) Zanolli, Z.; Onida, G.; Charlier, J.-C. *ACS Nano* **2010**, *4*, 5174.

(15) Cahangirov, S.; Topsakal, M.; Ciraci, S. *Phys. Rev. B* **2010**, *82*, 195444.

(16) Janowska, I.; Vigneron, F.; Bégin, D.; Ersen, O.; Bernhardt, P.; Romero, T.; Ledoux, M. J.; Pham-Huu, C. *Carbon* **2012**, *50*, 3106.

(17) Svensson, K.; Jompol, Y.; Olin, H.; Olsson, E. *Rev. Sci. Instrum.* **2003**, *74*, 4945.

(18) Golberg, D.; Mitome, M.; Kurashima, K.; Bando, Y. *J. Electron Microsc.* **2003**, *52*, 111.

(19) Ren, B.; Picardi, G.; Pettinger, B. *Rev. Sci. Instrum.* **2004**, *75*, 837.

(20) Campos, L. C.; Manfrinato, V. R.; Sanchez-Yamagishi, J. D.; Kong, J.; Jarillo-Herrero, P. *Nano Lett.* **2009**, *9*, 2600.

(21) Jhon, Y. I.; Zhu, S.-E.; Ahn, J.-H.; Jhon, M. S. *Carbon* **2012**, *50*, 3708.
(22) Qi, Z.; Zhao, F.; Zhou, X.; Sun, Z.; Park, H. S.; Wu, H. *Nanotechnology* **2010**, *21*, 265702.
(23) Erdogan, E.; Popov, I.; Rocha, C.; Cuniberti, G.; Roche, S.; Seifert, G. *Phys. Rev. B* **2011**, *83*, 041401.
(24) Marques, M. A. L.; Troiani, H. E.; Miki-Yoshida, M.; Jose-Yacaman, M.; Rubio, A. *Nano Lett.* **2004**, *4*, 811.
(25) Banhart, F.; Kotakoski, J.; Krasheninnikov, A. V. *ACS Nano* **2011**, *5*, 26.
(26) Nair, A. K.; Cranford, S. W.; Buehler, M. J. *Europhys. Lett.* **2011**, *95*, 16002.
(27) Akdim, B.; Pachter, R. *ACS Nano* **2011**, *5*, 1769.
(28) Onida, G.; Reining, L.; Rubio, A. *Rev. Mod. Phys.* **2002**, *74*, 601.
(29) van Schilfgaarde, M.; Kotani, T.; Faleev, S. *Phys. Rev. Lett.* **2006**, *96*, 226402.
(30) Meunier, V.; Sumpter, B. G. J. *Chem. Phys.* **2005**, *123*, 024705.
(31) Rangel, T.; Ferretti, A.; Trevisanutto, P. E.; Olevano, V.; Rignanese, G. M. *Phys. Rev. B* **2011**, *84*, 045426.
(32) Shen, L.; Zeng, M.; Yang, S.-W.; Zhang, C.; Wang, X.; Feng, Y. *J. Am. Chem. Soc.* **2010**, *132*, 11481.
(33) Ravagnan, L.; Manini, N.; Cinquanta, E.; Onida, G.; Sangalli, D.; Motta, C.; Devetta, M.; Bordoni, A.; Piseri, P.; Milani, P. *Phys. Rev. Lett.* **2009**, *102*, 245502.
(34) Paulson, M.; Krag, C.; Frederiksen, T.; Brandbyge, M. *Nano Lett.* **2009**, *9*, 117.
(35) Kim, K.; Sussman, A.; Zettl, A. *ACS Nano* **2010**, *4*, 1362.
(36) Balandin, A. A.; Ghosh, S.; Bao, W.; Calizo, I.; Teweldebrhan, D.; Miao, F.; Lau, C. N. *Nano Lett.* **2008**, *8*, 902.
(37) Banhart, F. *Rep. Prog. Phys.* **1999**, *62*, 1181.
(38) Russo, C. J.; Golovchenko, J. A. *Proc. Natl. Acad. Sci. U.S.A.* **2012**, *109*, 5953.
(39) Meyer, J.; Eder, F.; Kurasch, S.; Skakalova, V.; Kotakoski, J.; Park, H. J.; Roth, S.; Chuvilin, A.; Eyhusen, S.; Benner, G.; Krasheninnikov, A. V.; Kaiser, U. *Phys. Rev. Lett.* **2012**, *108*, 196102.
(40) Kotakoski, J.; Santos-Cottin, D.; Krasheninnikov, A. V. *ACS Nano* **2012**, *6*, 671.
(41) Standley, B.; Bao, W.; Zhang, H.; Bruck, J.; Lau, C. N.; Bockrath, M. *Nano Lett.* **2008**, *8*, 3345.

dx.doi.org/10.1021/nl4018918 | *Nano Lett.* XXXX, XXX, XXX−XXX